Deep Mining 2024 – P Andrieux & D Cumming-Potvin (eds)
© 2024 Australian Centre for Geomechanics, Perth, ISBN 978-0-6450938-9-6
doi:10.36487/ACG_repo/2465_93

Three-dimensional modelling of de-stressed rock mass using classification systems

Shahé Shnorhokian [a,*], Samar Ahmed [b]

[a] *Department of Mining and Materials Engineering, McGill University, Canada*

[b] *Department of Mining, Petroleum and Metallurgical Engineering, Cairo University, Egypt*

Abstract

De-stressing and preconditioning blasts have been used in the past 70 years at underground mines on all continents. The main design approach for implementing the technique has been empirical in nature and an engineering assessment methodology was developed only at the turn of the century. As mining progresses to increasing depths, additional tools are required to evaluate the impact of various de-stressing techniques and designs. Numerical modelling has been adopted since the early 1970s to simulate de-stressed rock masses and to aid in the assessment of the resulting stress distributions. In most cases, a percentage reduction (often by an arbitrary quantity) in the deformation modulus E_{rm} has been used to represent the de-stressed regions. Rock fragmentation and stress dissipation factors have constituted another approach used in modelling the affected areas.

In this paper, the rock mass rating (RMR) classification scheme is used as the basis for determining model input properties for de-stressed regions. Based on an extensive literature review, it is shown that the two main mechanisms responsible for de-stressing are the creation of new fractures or slippage of blocks on pre-existing ones. The RMR allocates 20 points each to the rock quality designation (RQD) and spacing of discontinuities, which can be incrementally reduced to account for the first mechanism. The conditions of discontinuities constitute another 30 points that can be used to adequately represent the second mechanism. Using a simplified 3D model of a typical mine in the Canadian Shield, the E_{rm} is calculated at an underground drift and crosscut system based on relative reductions in the RMR corresponding to both de-stressing mechanisms. Not only is the new approach found to be suitable for design purposes by validating it against reported field measurements, but the changes in the rock mass classification represent physical modifications that can be observed and that make sense from a rock mechanics perspective.

Keywords*: de-stressing, 3D modelling, rock mass classifications, deep mining*

1 Introduction

The consensus within industrial, governmental, and academic circles is that the future of underground mining is at increasing depth (Fairhurst 2017; Wagner 2019). Some of the deepest operations are already planning for mining geologic extensions to the orebodies being currently extracted. While there are multiple operational challenges to mining at significant depths, the key one associated with rock mechanics is the presence of extremely high in situ stresses. One of the techniques that has historically been implemented is the use of special blasts to de-stress or precondition the rock mass. Despite its having been applied since the 1930s and an assessment methodology having been developed in the first decade of the 21st century, the exact mechanisms involved are still not well understood. According to a categorisation adopted by many authors (Willan et al. 1985; McMahon 1988; Andrieux et al. 2004; Saiang & Nordlund 2005; Konicek et al. 2014, among others), de-stressing fractures and weakens the rock mass in areas where elevated stresses already exist, while preconditioning implements the same where future stress concentrations are anticipated. The authors recently

* Corresponding author. Email address: shahe.shnorhokian@mcgill.ca

published a comprehensive literature review on de-stressing and preconditioning applications in underground hard rock mines, in collieries with hard coal seams or competent roof formations, and in caving mines (Shnorhokian & Ahmed 2024).

Based on theoretical postulations and in situ measurements or observations, two main mechanisms have been put forward to explain the phenomenon of de-stressing. The creation of new fractures (or densification of existing networks) and slippage along pre-existing planes of weakness have constituted the two prevailing schools of thought. They were initially thought to be mutually exclusive but were later deemed to act in a complementary manner; multiple field observations and measurements in different mines have supported the presence of both mechanisms. The application of the technique in other geologic settings or to attain other objectives (such as in coal mines or for failure propagation and fragmentation improvement in caving mines, respectively) were observed to generate similar effects to classical de-stressing in hard rock metal mines. It was observed that in the latter geologic environment, stress drops of 6–19 MPa were typically measured, closure rates of around 1 cm were registered, and seismicity velocities decreased by 16–30%. Rock mass properties were altered with the modulus loss having a very wide range of reduction of 10–95%, and the intact rock strength was affected as indicated by lower unconfined compressive strength (UCS) values. In preconditioning applications, where hydraulic fracturing was used in caving mines, the percentage loss in rock mass strength was at the lower end of the spectrum previously established.

1.1 Overview of modelling techniques for de-stressed rock mass

Different techniques have been reported in the literature with respect to the modelling of de-stressed rock mass in underground mines. Examples include:

- the use of an in-house 3D elastic, boundary element code to determine the sequence of slot excavation between levels 6600–7000, and the total volume of de-stressed rock mass at the Creighton mine (Wiles & MacDonald 1988)
- a general finite element approach to examine the effect of a 1.8 m thick reef extraction on the de-stressing of the overlying rock mass in South African mines at 3,200 m depth (Whittaker & Reddish 1990)
- a simplified 2D finite element model to evaluate shaft stability in the Coeur d'Alene district (CDA) (Corp 1980)
- a displacement discontinuity, viscoplastic interface model to study the time-dependent growth of fractures resulting from preconditioning at the Blyvooruitzicht mine (Malan & Spottiswoode 1997).

With their gradual availability around the turn of the century, commercial codes replaced the individually developed ones or programmed software. Displacement discontinuity codes DZTAB and NFOLD 3D were used at the Macassa mine for modelling pre-de-stressed and post-de-stressed conditions, concentrating on the post-peak properties of the rock mass to obtain results comparable to field observations (Hanson et al. 1987). FLAC (finite difference) and MUDEC (distinct element) were used to verify stress and displacement values at the Pyhäsalmi mine before implementing de-stress slotting (Antikainen 1990). A special detailed review of techniques in numerical modelling for de-stress blasting noted some inherent limitations of this approach (Andrieux 2005). It should be mentioned that specialised codes and software to dynamically simulate de-stress blasts and the ground response from them are not covered in the current study, and the focus is on the simulation of already de-stressed or preconditioned rock mass.

During the second decade of the 21st century, further advances in numerical codes allowed for the use of more sophisticated modelling approaches for de-stressed rock mass. In an overview of the literature with respect to the use of controlled blasting for enhancing safety, the adoption of the Hybrid Stress Blasting Model to assess the zone affected by preconditioning blasts was presented (Toper et al. 1998; Sellers 2011). Map3D was also used to study the potential failure mechanism of the I1 rib pillar at the Mt Charlotte mine before implementing de-stressing (Mikula et al. 1995). Another study was conducted there with the same code for the planning of tight slot de-stressing in the ROB5 remnant pillar, and to assess the potential for

triggered fault slips and energy releases (Mikula et al. 2005). The inelastic version of Abaqus was adopted to model the de-stressed condition of a stiff dyke and Map3D was used to analyse the displacement along it, with the conclusion that the structure required preconditioning for development to go through without incurring major seismic events (Sengani & Amponsah-Dacosta 2018; Sengani & Zvarivadza 2018). The references mentioned above are only some examples from the literature (among others) where different types of numerical codes have been used in connection to de-stressing.

Just as multiple codes have been used to simulate de-stressed rock mass, modelling approaches have also varied. Reductions in modulus have comprised the main technique, but others such as assigning relaxation factors have also been reported. More sophisticated methods have been suggested such as the use of 'strain cohesion softening-friction hardening' values based on adjusted triaxial results (James 1998). Another recommended approach has been implementing a progressive process whereby affected or de-stressed material is gradually replaced and softened at each stage (Vlachopoulos & Diederichs 2014).

1.2 Quantitative reductions in rock mass properties

In addition to the general use of numerical models, authors have reported quantitative reductions in rock mass properties when used as input parameters for de-stressed regions. In studies where field test measurements were obtained, these have been introduced into the model directly. In other cases where conceptual models were simulated, the changes have been based on previous studies or the authors' judgement. A few examples can be cited here from a much larger literature on the topic. In a 2D finite element modelling for the 40-135E stope at the Galena mine in the CDA district and based on seismic velocity surveys, reductions were made in both the rock mass modulus and Poisson's ratio. Fractured areas were represented with a modulus of 6,895 MPa compared to the original 80,670 MPa, the Poisson's ratio was modified from the original 0.19 to 0.25, and the UCS was reduced from 174 MPa to 0 (Blake 1972a). In a second study of a diminishing sill pillar at the same mine, the maximum principal stress attained values of 244 MPa when its thickness approached 9 m. A de-stressed version of this pillar was modelled by reducing the orebody modulus from 39,645 to 6,895 MPa, which represented 17% of the original value (Blake 1972b). In a related study at the Star-Morning mine, fractured and de-stressed rock mass was also simulated in 2D using a modulus of 6,895 MPa and 3,447 MPa instead of the original 25,855 MPa, with the Poisson's ratio changing from 0.2 to 0.25 (Karwoski et al. 1979). The study of de-stress slotting in the footwall roof at the Näsliden mine was simulated with a 2D finite element model where the properties in the slot were reduced to 2.5, 5, and 10% of the original modulus, resulting in a reduction of up to 60% in the horizontal stresses (Krauland & Söder 1988). A 3D finite-boundary element model was used to verify the effect of another de-stress slot at the Malmberget mine where the modulus was varied between 12 and 28 GPa compared to the original 40 GPa of the rock mass (Borg 1988).

At the Red Lake mine in Canada, NFOLD displacement discontinuity and finite element modelling were used to simulate de-stressing. The rock mass modulus was reduced by 25 and 50% to replicate the de-stressed zones, which agreed reasonably well with the installed instrumentation (Makuch et al. 1987). In addition, 2D finite element modelling was adopted to determine the required reduction in modulus to represent de-stressed field conditions (Scoble et al. 1987). Assessing the 25 and 50% reduction results in the model, monitored field stress changes of around 5.5 MPa and closures of up to 3 mm were deemed to be closer to the latter. Another displacement discontinuity modelling study was conducted to predict the location of potential bursting in the 1604E stope at the Red Lake mine and to compare the effects of de-stressing. Sample closure and stress change data after the blast was compared to 2D model predictions and the indication was a reduction of 50% in the rock mass modulus (Cullen 1988). NFOLD was used at the Macassa mine on L 5725 to model a de-stressed crown pillar and it was observed that the modulus required a 67% reduction to match field observations (Hedley & Udd 1989). Apart from the displacement discontinuity approach, the finite difference code FLAC was used in a 2D conceptual study of de-stressing in development heading shoulders and backs. To achieve the stress transfer required, the bulk and shear moduli were reduced, as well as the friction angle, to 50% of their original values, with the cohesion set to zero (Hedley 1992). Both 2D and 3D boundary element modelling were used to study the impact of a de-stress cut at the South Deep mine, and

the fractured zone was simulated by reducing the rock mass rating (RMR) from 82 to 53, using a modulus of 10 GPa instead of the original 64 GPa, and reducing the bulk (K) and shear (G) moduli from 45.38 and 25.19 GPa to 8.86 and 4.67 GPa, respectively (James 1998).

Within the category of in-house codes, the 2D finite element code MSAP2D was used to conceptually model a steeply dipping 3 m wide vein being mined with the overhand cut-and-fill method in the Canadian Shield. To simulate the de-stressed rock mass, its modulus was reduced from 80,700 to 8,070 MPa, which was 10% of the original value. In addition, the Poisson's ratio was increased from 0.22 to 0.25, the cohesion was reduced from 25 to 15 MPa, and the friction angle was modified from 35° to 25° (Mitri et al. 1988). Another 2D linear elastic conceptual modelling of a 5 m wide, steeply dipping orebody using the cut-and-fill method was examined and regions of de-stressed rock mass in the orebody, footwall, and hanging wall had their modulus and the Poisson's ratio reduced to 20% of their original values. Based on the results, it was observed that stresses were reduced by 50%, and the conclusion was that a de-stressed zone would have 10-50% of the original modulus value of the rock mass. Significantly, it was determined that simply reducing the rock mass properties of the modelled region was not enough to generate a decrease in stresses but that a manual reduction should also be implemented by the user (Momoh et al. 1996).

The advanced 3D discontinuum discrete element code 3DEC was used for de-stressing analysis in the 29-9 pillar at the Brunswick mine (Andrieux et al. 2003). The strain softening constitutive model was used and two approaches to simulate the de-stressed rock mass were adopted. Firstly, the stiffness was reduced by 10 and then 50%, which did not provide matching results to the stress drops measured at the mine. Secondly, the de-stressed rock mass was numerically removed, and a much better agreement was observed between model and instrumentation readings (Andrieux et al. 2003). Map3D was used to model tight slot de-stressing at the Mt Charlotte mine and the modulus reductions implemented for representing the affected zone ranged 0–6.5 GPa compared to the original 65 GPa (Mikula et al. 2005). The code was also used for modelling a de-stress blast in the I1 rib pillar at the same mine and results indicated a change in the magnitude and orientation of stresses after the blast, with a reduction from 65 to 11 GPa in the pillar modulus (Mikula & Lee 2002). In another study, reduced cohesion and friction angles were used to represent a preconditioned drift in 3D, along with 10–40% reductions in the modulus and an increase of the Poisson's ratio from 0.28 to 0.35–0.40 (Yu et al. 2021).

In coal mines, RS2 has been used to examine stresses in the roof at Lazy, Dubrava, and ČSA, specifically to compare them without and with de-stressing being applied. At the Lazy mine, a modulus of 250 MPa and a Poisson's ratio of 0.40 were used to represent completely fractured and caved rock mass at locations where bursting had taken place in longwall no. 140704 (Konicek et al. 2014; Konicek & Waclawik 2018). The 2D discrete element code UDEC was adopted to study the effect of hydraulic fracturing in a typical coal section with the cohesion and tensile strengths reduced to zero and the friction angle set at 20° to represent fractured rock mass due to de-stressing (Kang et al. 2018).

Apart from reductions in RMR, modulus, Poisson's ratio, UCS, cohesion, and internal angle of friction, several authors have used the concept of blast-induced damage to provide weaker properties for de-stressed rock mass. For example, the blast damage factor D (Hoek et al. 2002) has been adopted in several modelling studies, as well as reduced intact rock mass properties and Geological Strength Index (GSI) values (Torbica & Lapčević 2015; Jessu et al. 2018). A parametric study was conducted where factor D ranges of 0.25–1 were used in conjunction with a bilinear strain softening model to simulate blast-damaged rock mass for pillar stability analysis in FLAC3D (Jessu et al. 2018).

1.2.1 Rock fragmentation (α) and stress dissipation (β) factors

Within the literature of quantitative reductions in properties, a technique adopting rock fragmentation (α) and stress dissipation (β) factors was also developed (Mitri et al. 2000; Tang 2000). The rock fragmentation factor was introduced to implement a reduction of the rock mass modulus in the model after de-stressing, a phenomenon that had been reported by multiple authors. To account for de-stressing due to block slippage on discontinuities where no modulus reduction was required, the authors also introduced the stress

dissipation factor to initiate changes in model readings after de-stressing. They were implemented for two de-stressing patterns around a conceptual drift typically found in Canadian mines, using α and β values of 0.4 (Mitri et al. 2000). This approach was then used for several conceptual studies in 2D and 3D, including a model to study de-stressing work conducted in the 1902 and 1802 crown and sill pillars at the Campbell mine where an average α of 0.5 and a β of 0.6 were derived (Tang 2000). Apart from Canadian mines, the same technique was adopted for a back-analysis of the Star-Morning mine (Mitri 2000). While the primary objective of the factor α was to reduce the rock mass modulus, it was also applied to the Poisson's ratio (Tang & Mitri 2001). In later studies, the importance of directional fracture growth was underlined for rock mass under confinement (Saharan 2004). Multiple combinations of α and β were used in FLAC3D to model a conceptual de-stress panel and create a stress shadow for an ore pillar (Vennes & Mitri 2017). A 10–30% immediate reduction in stresses was obtained using a combination of α = 0.1 and β = 0.9 and a holistic approach was used where the sum of the two factors was assumed to be unity (Vennes et al. 2020). FLAC3D was adopted to study a large-scale de-stressing programme in the 100 orebody at Copper Cliff mine, which was calibrated based on readings from uniaxial stress sensors, and resulted in a combination of α = 0.05 and β = 0.95 to provide the best overall results (Vennes et al. 2020). Table 1 presents a selection of changes in input parameters from the literature that were implemented to represent de-stressed rock mass.

Table 1 Selected references where input parameters were modified to represent de-stressed rock mass

Mine/model	Reference	E_{rm}	K, G	ν	RMR	D	α/β
Campbell	Tang (2000)	–	–	–	–	–	0.5/0.5
Chengzhuang	Zhu et al. (2013)	3,000 to 30 MPa	–	–	–	–	–
Conceptual	Hedley (1992)	–	50%	–	–	–	–
Conceptual	Jessu et al. (2018)	–	–	–	–	0.25 to 1	–
Conceptual	Mitri et al. (2000)	–	–	–	–	–	0.4/0.4
Conceptual	Momoh et al. (1996)	50–90%	–	80%	–	–	–
Conceptual	Vennes & Mitri (2017)	–	–	–	–	–	0.1/0.9
Copper Cliff	Vennes et al. (2020)	–	–	–	–	–	0.05/0.95
Galena	Blake (1972a, 1988)	79.29 to 6.89 GPa	–	0.19 to 0.25	–	–	–
Galena	Boler & Swanson (1993)	50%	–	–	–	–	–
Huize	Yu et al. (2021)	10–40%	–	0.28 to 0.4	–	–	–
Macassa	Hedley & Udd (1989)	67%	–	–	–	–	–
Malmberget	Borg (1988)	40 to 12–28 GPa	–	–	–	–	–
Näsliden	Krauland & Söder (1988)	2.5, 5, 10%	–	–	–	–	–
Red Lake	Makuch et al. (1987); Scoble et al. (1987); Cullen (1988)	25–50% of 95 GPa	–	0.23	–	–	–
South Deep	James (1988)	64 to 10 GPa	K: 45.38 to 8.86 GPa; G: 25.19 to 4.67 GPa	–	82 to 53	–	–
Star-Morning	Karwoski et al. (1979)	25.9 to 6.9 and 3.5 GPa	–	0.2 to 0.25	–	–	–

As an overall summary for this section, modulus reductions of at least 50% have been required to calibrate a model with field observations. The Poisson's ratio has been modified in only a few studies with a general increase of 10% in value to render the rock mass softer. The α and β factors have varied between average values initially and minima-maxima in recent studies.

2 Rock mass classifications, de-stressing, and modelling

Based on the reviewed literature, blast-induced de-stressing or preconditioning in rock masses result in a limited set of observable phenomena. While all of them are not present in each case, they are confined to the generation of new fractures, the densification and extension of pre-existing fractures, forced slippage on pre-existing fractures that may include shearing of asperities and an increase in aperture or dilation of pre-existing fractures. Similarly, field observations of the impacts of successful de-stressing or preconditioning can be described as the softening or weakening of the rock mass, lowering of its deformation modulus E_{rm}, a reduction in stresses, the release of accumulated strain energy, an increase in convergence and/or closure and their rates, and a decrease in the magnitude and frequency of seismicity. However, modelling techniques adopted for de-stressed rock masses are not correlated quantitatively with geologic or rock mechanics observations in the field. The modulus reduction approach is used almost ubiquitously but it is rarely quantified based on actual measurable changes in the rock mass. Rather, a simple percentage reduction is applied to it until the model results are comparable to field observations. Since there might be other unknown variables that are responsible for differences between field and model readings, the modulus adjustment might result (unbeknownst to the researcher) in assigning the full weight of all discrepancies to that single parameter.

The new approach introduced here assigns reduced model input properties of de-stressed regions based on rock mass classification systems or related parameters, which can be measured or observed in the field. The novelty is in the quantitative effect of using a reduced classification number to represent a decrease in E_{rm} in de-stressed areas, and its comparison to assessments from field monitoring. Furthermore, since formations in most mines are already classified using these systems, the approach represents continuity in the methodology and makes sense from a rock mechanics perspective.

2.1 Rock mass rating (RMR)

The RMR classification system (Bieniawski 1976, 1989) is widely used in underground mining and allocates up to 70% of its value to fracture properties. In several studies, extensive analyses of the various interrelationships between classification systems comprising RMR, Q, modified Q', and GSI were conducted. As a conclusion, several equations were recommended for conversions between RMR and modified Q', as well as to calculate the E_{rm} value (Ahmed 2011; Russo & Hormazabal 2019). Since all these relationships are empirical in nature and are based on different datasets, the formulas by Hoek & Brown (1997) and Hoek & Diederichs (2006) will be adopted in this paper to provide analytical uniformity. Apart from these relationships, the modulus of the rock mass (P1) and degree of fracturing (P4) needed in the Destressability Index approach could also be related to the RMR value, although this is used for calculations prior to the blast taking place (Andrieux et al. 2004; Andrieux & Hadjigeorgiou 2008). The relationship between RMR and GSI is presented in Equation 1 based on the formula by Hoek & Brown (1997).

$$GSI = RMR - 5 \quad (1)$$

where:

GSI = geological strength index.

RMR = rock mass rating.

The E_{rm} can then be calculated using the formula proposed by Hoek & Diederichs (2006) (Equation 2) where the GSI and damage factor D are combined with the intact modulus E_i.

$$E_{rm} = E_i\{0.02 + \frac{1-\frac{D}{2}}{1+e^{\left[\frac{60+15D-GSI}{11}\right]}}\} \quad (2)$$

where:

E_{rm} = rock mass or deformation modulus

E_i = modulus of intact rock sample

D = blast damage factor

GSI = geological strength index.

In the final step, the bulk (K) and shear (G) moduli can be calculated using the E_{rm} and Poisson's ratio (ν) (Equations 3 and 4).

$$K = \frac{E}{3(1-2\nu)} \quad (3)$$

$$G = \frac{E}{2(1+\nu)} \quad (4)$$

The RMR system allocates various percentages to the effects of rock quality designation (RQD), spacing of discontinuities, and their conditions in terms of roughness, separation, or weathering. The total for a perfect rock mass is 100 points, out of which 70 originate from these three properties. If a rock mass were classified prior to and after de-stress blasting, its RMR value would not remain the same. While artificial fractures that result from drilling are not part of the usual RQD or RMR classification schemes, intentional blast-induced damage in the rock mass does not fall within that category. Firstly, the purpose of discounting artificial fractures due to drilling is to avoid designating the rock mass to be weaker than it is beneath the ground surface. With de-stressing, the rock mass does indeed become weaker and softer as observed by multiple authors (e.g. Board & Fairhurst 1983; Scoble et al.1987; Mikula et al. 1995; Andrieux et al. 2003; Hashemi & Katsabanis 2021) and new fractures are generated in it. Secondly, the rock mass that is damaged due to de-stressing is unable to carry elevated stresses, a limitation shared with a natural formation of comparable fracture density. Thirdly, a modelling code does not comprehend the differences between natural and blast-induced fractures within the RQD system. However, it requires a modified input based on these parameters that describes a weaker rock mass and allows it to generate lower stresses accordingly. Based on the RMR classification system, the effect of de-stress blasting can be quantified by one or more of the three properties mentioned above. It should be noted that stress-induced fractures generated between the excavation and de-stressing stages are not considered here. The reasoning would be that if they were present in sufficient density, they would partially dissipate the elevated stresses and there would not be a need for de-stressing.

As an example, a class II (good rock) rock mass with an RMR of 79 is considered prior to de-stress blasting. The total score is the sum of an intact UCS of 150 MPa (12 points), an RQD of 80% (17 points), and a single set of discontinuities spaced at 1 m (15 points), which can be described as less than a metre in length. Their surfaces are slightly weathered and rough, having less than 0.1 mm separation (25 points), and are under damp conditions (10 points). As a result of de-stress blasting, the intact UCS, weathering, and groundwater properties will remain the same in the short-term, and one or several others will change in the rock mass. The latter ones are first presented in the sections following, along with their specific changes in this example.

2.1.1 Rock quality designation

If new fractures are formed due to de-stress blasting, then it is obvious that the geologist or engineer logging the rock mass would assign a different de-stressed RQD value to it than the pre-de-stressed one. However, the effect would be minimal on the overall RMR value. If the new fracture density reduces the RQD from 80% to 45%, for example, only four points are lost from the total RMR score. In the example prior, if new fractures are formed and 20 cm of core per 1 m loses lengths more than 10 cm, then the $RQD_{de\text{-}stress}$ will be reduced to 60% and the $RMR_{de\text{-}stress}$ changes to 75 due to the loss of four points.

2.1.2 Spacing of discontinuities

Newly formed fractures (assuming that they are aligned parallel to the natural ones due to the same geologically induced defects in the rock mass) would have a significant impact on the rating allocated to their spacing. Even when this is only reduced to 0.5 m from an original 1 m, five points are deducted from the RMR score for this property alone. A closer spacing (0.06–0.2 m) could result from a second set of fractures generated at an angle to the first one, which would deduct seven points instead of five. Since the difference is relatively small, the five point deduction is considered for simplification. Combined with another potential four points from the RQD value, it would result in a total reduction of nine points. In the example prior, if only the spacing of fractures is reduced to 0.5 m from an original 1 m, the $RMR_{de\text{-}stress}$ becomes 74 due to the loss of five points.

2.1.3 Condition of discontinuities

The RMR score is most sensitive to the condition of discontinuities in the rock mass after de-stressing. Several authors (e.g. Toper et al. 1997; Swedberg et al. 2018; Konicek et al. 2019) have reported that blasting forces slippage on existing fractures, sometimes breaking the jagged surficial features that had been interlocking the blocks together up to that point. In addition, gaseous expansion from blasts have been reported to separate blocks along existing fractures (e.g. Cullen 1988; Grodner 1999; Sengani et al. 2019), thus dilating them and increasing the aperture in between. Up to five points can be lost due to a change from a slightly rough and weathered fracture surface with less than 1 mm of aperture and no infill, to a 2 mm one that is allowed to slip since the surface roughness would also be rendered ineffective with dilation. In the example above, if only the aperture separation of blocks increases from 0.1 to 1.5 mm, the $RMR_{de\text{-}stress}$ becomes 75 due to the loss of four points. However, this separation will directly affect the surface roughness parameter as well since it can no longer be relied upon to provide resistance to movement. Hence, an additional 2-3 points could be lost for a maximum total of seven points, bringing the $RMR_{de\text{-}stress}$ down to 72.

2.1.4 Combined effect

The combination of any two or all three of the factors outlined prior would result in an even more significant reduction in the $RMR_{de\text{-}stress}$ value. In the example, if all three properties change simultaneously, then the $RMR_{de\text{-}stress}$ is reduced from the original 79 to 63 for a total maximum drop of 16 points.

2.1.5 Reduction in deformation modulus

It would be instructive to quantify the impact of these reductions on the rock mass deformation modulus. Using the conversion formula from RMR to GSI (Hoek & Brown 1997) and the relationship by Hoek & Diederichs (2006), the results would be as follows:

- RMR 79: in the original rock mass, the E_{rm} is 119.3 GPa, which translates into a bulk modulus K of 76.5 GPa and a shear modulus G of 48.1 GPa.
- $RMR_{de\text{-}stress}$ 74: if only the RQD or spacing properties change, the lowest $E_{rm\ de\text{-}stress}$ will be 106.4 GPa, with $K_{de\text{-}stress}$ = 68.1 GPa and $G_{de\text{-}stress}$ = 42.9 GPa.
- $RMR_{de\text{-}stress}$ 72: if only the condition of discontinuities changes, the lowest $E_{rm\ de\text{-}stress}$ will be 100.4 GPa, with $K_{de\text{-}stress}$ = 64.4 GPa and $G_{de\text{-}stress}$ = 40.5 GPa.
- $RMR_{de\text{-}stress}$ 63: if all three properties change simultaneously, the $E_{rm\ de\text{-}stress}$ becomes 70.7 GPa, with $K_{de\text{-}stress}$ = 45.3 GPa and $G_{de\text{-}stress}$ = 28.5 GPa.

It can be observed that the quantitative physical changes due to de-stress blasting have varying impacts on the input parameters typically used in numerical modelling codes. With all three properties changing at the same time, the $E_{rm\ de\text{-}stress}$ can easily diminish to about 59% of its original value. However, it is also shown that only increasing apertures of existing fractures through explosive gas pressure reduces the same parameter to 84% of the original deformation modulus.

2.2 Numerical modelling

To evaluate the newly introduced approach of quantitatively reducing the E_{rm} of de-stressed rock masses based on the RMR system, a simplified model of a typical underground mine in the Canadian Shield was constructed in FLAC3D (Itasca Consulting Group Inc 2019). It comprises a tabular orebody striking north–south and dipping steeply within a host greenstone formation. Two parallel dykes are present on either side of the orebody, with a norite unit further to the north and metasediments to the south. Haulage drift systems with north, central, and south crosscuts are included in the footwall (north) and hanging wall (south) sections of the greenstone formation on four levels: L 1460, L 1490, L 1520, and L 1550. Figure 1a presents an isometric view of the model and Figure 1b provides a closer view of the studied drifts on L 1490 and L 1520. In Figure 2, the geologic formations and the dimensions of the orebody are provided for L 1490.

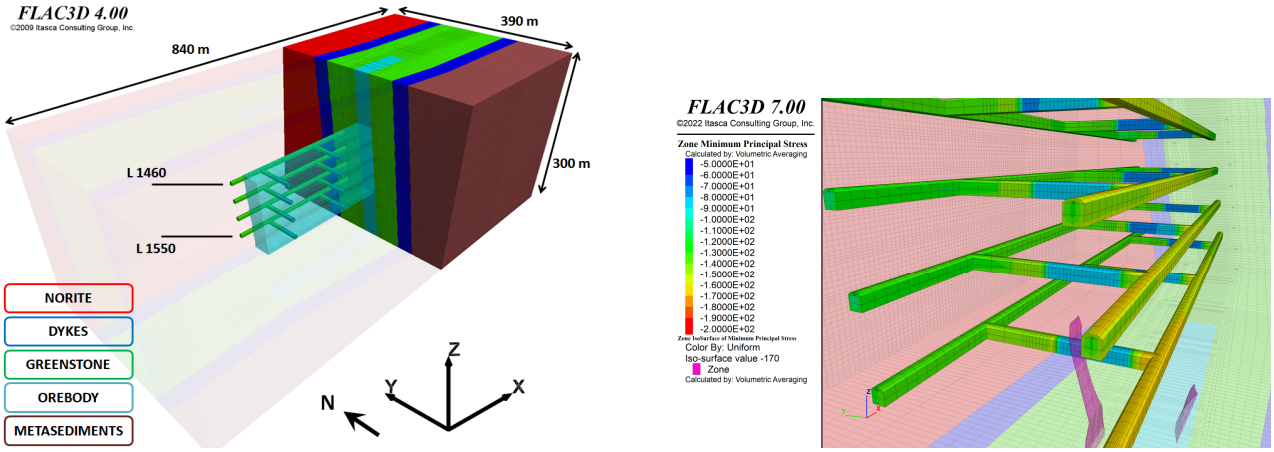

(a) (b)

Figure 1 Isometric views of the numerical model. (a) Overview of levels; (b) Drifts on L 1460, L 1490, L 1520, and L 1550

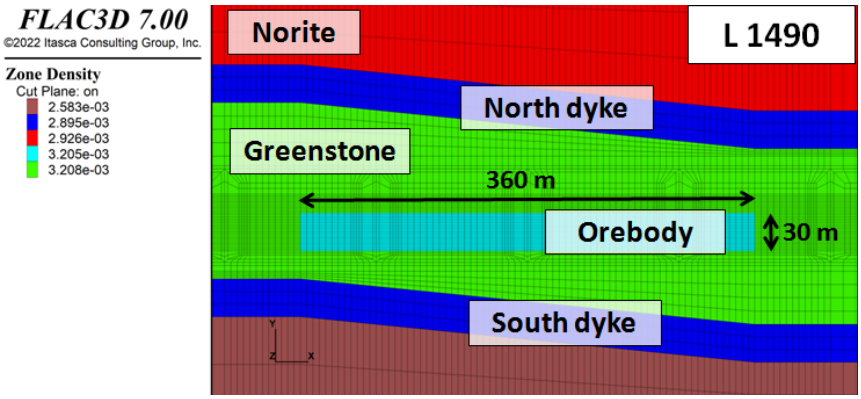

Figure 2 Geologic formations and orebody dimensions on L 1490

Rock mass properties from a previous case study were adopted and pre-mining stresses were generated using boundary tractions. Both drift systems were partially and simultaneously excavated in five 5 m advances to assess induced stresses on the development faces. Two identical models were used with different RMR values assigned to the drifts on L 1490 and L 1520 based on the example above, while the ones on L 1460 and L 1550 retained their original values. In the first baseline model, RMR 79 was used and the E_{rm}, K, and G values were calculated according to the formulas presented previously. In the second case, $RMR_{de\text{-}stress}$ 63 was assumed to represent a combination of new fracture formation and slippage on pre-existing ones. The model input properties are presented in Table 2 and the simulation was done in linear elastic mode to provide maximum stress magnitudes.

Table 2 Input parameters for the baseline and de-stressed models

Geologic unit	E_i (GPa)	ν	Baseline RMR	E_{rm} (MPa)	$RMR_{de\text{-}stress}$	$E_{rm\ de\text{-}stress}$ (MPa)
Norite	178	0.21	59	69,234	59	69,234
Dyke	126	0.24	63	58,816	63	58,816
Greenstone	149	0.24	79	119,380	63	70,726
Metasediments	77	0.29	55	23,127	55	23,127
Orebody	69	0.30	75	50,564	75	50,564

3 Results and discussion

The focus of this study was an analysis of the maximum stress magnitude obtained in the drift face prior to and during the various stages of excavation. Hence, the major principal stress (σ_1) was monitored and comparisons drawn between values obtained in each stage within the two models. It should be noted that an examination of the minor principal (σ_3) and differential (σ_1–σ_3) stresses would yield a more comprehensive assessment of the mechanisms of de-stressing, which will be the focus of an upcoming publication by the authors. In this study, σ_1 was the basis of comparisons between the two models for each stage of excavation to evaluate the merits of de-stressing.

3.1 Baseline model – RMR 79

In Figure 3, stresses at and around the south drift face are presented in isometric view for the pre-excavation, first, and fifth stages of development in the baseline model, focusing on L 1490 and L 1520 in the centre. A σ_1 isosurface for 170 MPa is also plotted to monitor areas of extremely elevated stresses. As mentioned before, the implementation of de-stressing does not remove high stresses altogether but simply transfers them to another location. Hence, it would be of interest to identify those regions where this transfer is made to, with their absence probably indicating that the de-stressing application was unsuccessful. The pre-mining σ_1 magnitude on the south drift face on L 1490 is 156 MPa with 163 MPa registered along the drift axis behind it until the western crosscut intersection. This is a high stress region due to the proximity of the south dyke to the orebody as shown in Figure 2. It is precisely because of these high stresses that the south drift was selected for modelling the effects of de-stressing.

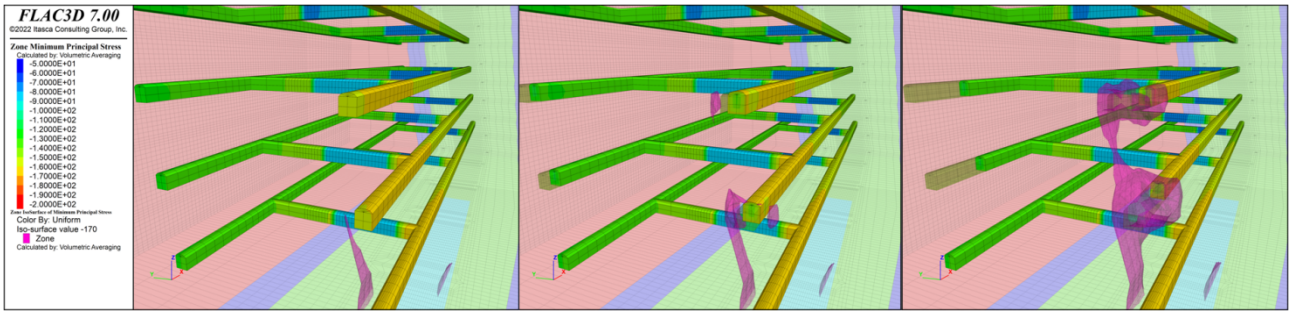

Figure 3 Baseline model (RMR 79) – pre-excavation, stage 1, and stage 3 magnitudes of σ_1, focused on L 1490 and L 1520 drift systems

On the other hand, the north drift indicates a σ_1 magnitude of 126 MPa with 134 MPa at the western crosscut intersection. Hence, there is a pre-excavation difference of around 30 MPa between the north and south drifts. With increasing depth, the σ_1 magnitude is slightly elevated to 158 MPa on L 1520 for the south drift but the western crosscut intersection remains at 163 MPa. A similar 3 MPa increase is observed for the north drift and intersection on L 1520.

At the first stage of excavation, the σ_1 magnitude on the south drift face on L 1490 decreases slightly to 145 MPa in its centre but remains elevated at 163 MPa along its boundaries and just behind it. Of note is the appearance of the 170 MPa σ_1 isosurface to the north of the drift, indicating that high stresses have moved from the excavated region to the adjacent rock mass. The importance of this mechanism was already mentioned above, but its appearance in the model validates that the simulation is representative of field conditions. A similar trend is also observed for the excavation of the south drift on L 1520. In the north drift, the σ_1 magnitude decreases to 115 MPa in the centre of its face, with the original 134 MPa still registering at its boundaries and behind it.

Similar trends are observed in the south and north drifts on L 1490 and L 1520 in stages 2, 3, and 4. By stage 5, the maximum σ_1 magnitude of 163 MPa dominates the south drift and 134 MPa prevails in the north one at every step of excavation. The notable difference is the increase in the 170 MPa σ_1 isosurface that envelopes the south drift and extends from L 1490 to L 1520. Hence, the practical aspect of the analysis is that developing the south drift will be conducted under high face stress conditions, which will also result in a significant volume of the adjacent rock mass being under a 170 MPa σ_1 stress regime.

3.2 De-stressed model – $RMR_{de\text{-}stress}$ 63

In Figure 4, stresses at and around the south drift face are presented for the pre-excavation, first, and fifth stages of development in the de-stressed model, focusing on L 1490 and L 1520. A σ_1 isosurface for 170 MPa is once again plotted to monitor areas of extremely elevated stresses. An immediate observation that can be made is that the pre-mining σ_1 magnitude on the south drift face on L 1490 now reads a maximum of 141 MPa along its boundary, with 148 MPa registered along the drift axis and at the western crosscut intersection. The σ_1 magnitude in the north drift reads 106 MPa in the face centre, and a maximum of 121 MPa appears around its boundaries and along the axis towards the western crosscut. It is therefore clear that de-stressed rock mass has been successfully simulated with a reduction in pre-excavation stress levels in both drift systems, reflecting values typically reported in the literature. The reduction of around 15–20 MPa matches the upper limits of typical stress drop ranges in field implementations of de-stressing, which reflect the combined mechanisms represented by an $RMR_{de\text{-}stress}$ of 63. It is also interesting to observe that the 170 MPa σ_1 isosurface is more voluminous on L 1520, thus indicating that the de-stressed status of the south drift has shifted the high stresses to the adjacent rock mass.

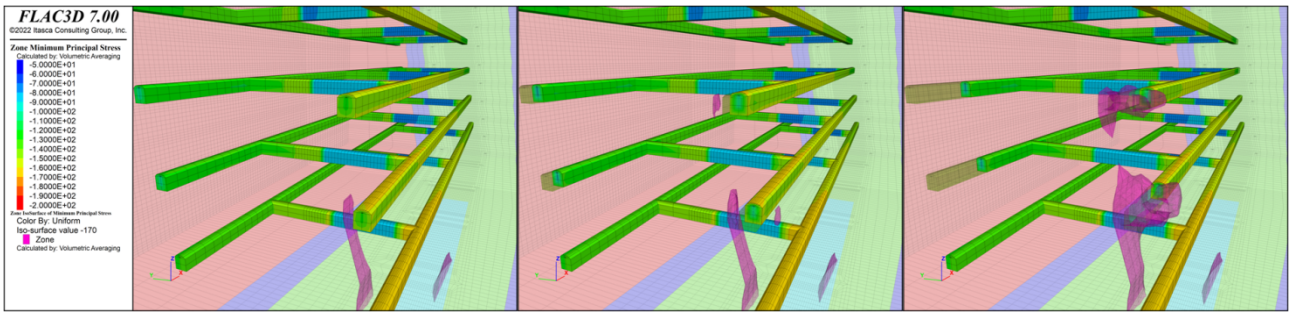

Figure 4 De-stressed model ($RMR_{de\text{-}stress}$ 63) – pre-excavation, stage 1, and stage 3 magnitudes of σ_1, focused on L 1490 and L 1520 drift systems

With the first stage of excavation, the centre of the south drift face indicates a σ_1 magnitude of only 90 MPa, with a maximum of 142 MPa appearing around the peripheries and increasing to 151 MPa behind it. As a minimum, a 10–15 MPa drop in the σ_1 value is observed at the locations of highest stress concentration around the south drift, with more significant reductions in the face centre. The 170 MPa σ_1 isosurface appears at this stage on L 1490 as with the baseline model, but its volume on L 1520 is less than before. This is due to the high stresses already having shifted to the adjacent rock mass before the excavation stages, which did not happen in the case of the baseline model. At stage 5, the established trends continue to persist on L 1490 and L 1520, and at both the north and south drift systems. The main observation is that the 170 MPa σ_1 isosurface does not connect the two levels as before and is less voluminous than the one in the baseline model at the same stage.

Due to the de-stressed state of both drift systems, all transfers were already completed prior to the excavation stage and minimal changes occurred afterwards.

3.3 Comparative analysis

It can clearly be observed that the de-stressed model provides a measurable reduction in maximum stress values on the drift faces before excavation commences. The lower magnitudes of σ_1 are within the range of measured reductions in stress found in the literature. Furthermore, this was achieved with a logical reduction in E_{rm} that was directly linked to the two main mechanisms of de-stressing postulated by various authors and verified by field observations, which are the creation of new fractures and slippage along pre-existing ones due to a reduction in their surface shear resistance. The new approach of correlating changes induced by de-stress blasting to a rock mass classification system provides multiple benefits. Firstly, it allows the determination of model input properties based on actual observable and quantifiable changes in the rock mass. This prevents oversimplified reductions in the deformation modulus values based on generalised percentages. However, it also requires specialised instrumentation to obtain details of fracture density and geometry. Secondly, it provides a possible explanation as to the contradictory reports on successful, moderate, and unsuccessful de-stressing tests in the literature. Depending on the blast design in the previous example, the E_{rm} can be reduced by up to 41% from its original value, which covers the entire range of field assessments made for de-stress blasts. Thirdly, it correlates well with the observations in the field that a combination of forming new fractures, slippage and shearing on pre-existing ones and rock block movements are key requirements for de-stressing as none of them alone reduces the E_{rm} by more than 16%.

4 Conclusion

In this study, a literature review on de-stressing of competent rock mass in underground mines indicated that its mechanisms congregated around two main schools of thought. In the first case, the generation of new fractures or the densification and extension of pre-existing ones were thought to release strain energy and move stresses into adjacent formations. In the second case, the shearing of asperities and dilation of pre-existing fractures were proposed to be responsible for de-stressing. A related review concluded that the main approach for simulating de-stressed rock mass, has been a reduction in the deformation modulus E_{rm} by using a generalised percentage that did not necessarily fit the geologic properties of the affected rock mass. A new quantitative approach was then proposed to simulate de-stressed rock mass based on classifications commonly used for characterisation in underground mines such as the RMR system, which allocated three quarters of its value to parameters affected by specialised blasting for this purpose. Using a simplified numerical model of a typical mine in the Canadian Shield, a comparison was made between the baseline simulation where no de-stressing was implemented and an identical one where a combination of new fractures and slippage on pre-existing ones occurred. A reduction in the major principal stress magnitude was observed in the latter, which was within the range typically reported from field applications. Furthermore, de-stressing the drifts transferred high stresses to the adjacent rock mass at the onset of excavations and provided improved ground conditions for development.

Acknowledgement

The authors would like to acknowledge Itasca for the provision of FLAC3D licenses through the Itasca Educational Partnership (IEP) Teaching Program to the Department of Mining and Materials Engineering at McGill University.

References

Ahmed, S 2011, *Assessment of Rock Mass Deformation Modulus Equations Using Monte Carlo's Statistical Simulation*, Masters thesis, Cairo University, Cairo.

Andrieux, PP 2005, *Application of Rock Engineering Systems to Large-Scale Confined Destress Blasts in Underground Pillars*, PhD thesis, Université Laval, Québec.

Andrieux, P & Hadjigeorgiou, J 2008, 'The destressability index methodology for the assessment of the likelihood of success of a large-scale confined destress blast in an underground mine pillar', *International Journal of Rock Mechanics and Mining Sciences*, vol. 45, no. 3, pp. 407–421. https://doi.org/10.1016/j.ijrmms.2007.07.006

Andrieux, PP, Brummer, RK, Liu, Q, Simser, BP & Mortazavi, A 2003, 'Large-scale panel destress blast at Brunswick mine', *CIM Bulletin*, vol. 96, no. 1075, pp. 78–87.

Andrieux, P, Hadjigeorgiou, J & Brummer, R 2004, 'A rock engineering systems approach to destress rock blasting', *Challenges in Deep and High Stress Mining*, in Y Potvin, J Hadjigeorgiou & TR Stacey (eds), Australian Centre for Geomechanics, Perth, pp. 479–486.

Antikainen, J 1990, 'Open stope design under adverse rock mechanical conditions at Pyhäsalmi Mine', *Rock Mechanics Contributions and Challenges Proceedings of the 31st US Symposium on Rock Mechanics,* CRC Press, Boca Raton, pp. 1013–1018.

Bieniawski, Z 1976, 'Rock mass classification in rock engineering applications', in ZT Bieniawski (ed.), *Proceedings of the Symposium on Exploration for Rock Engineering,* A. A. Balkema, Rotterdam, pp. 97–106.

Bieniawski, ZT 1989, *Engineering Rock Mass Classifications: A Complete Manual for Engineers and Geologists in Mining, Civil, and Petroleum Engineering*, Wiley, Hoboken.

Blake, W 1972a, 'De-stressing test at the Galena Mine, Wallace, Idaho', *Journal Transactions of the Society of Mining Engineers of AIME*, vol. 252, no. 3, pp. 294–299.

Blake, W 1972b, 'Rock-burst mechanics', *Q Colorado School of Mines*, vol. 67, pp. 1–64.

Board, M & Fairhurst, C 1983, 'Rockburst control through de-stressing – a case example', *Proceedings of the conference on Rockbursts – Prediction and Control*, Institute of Mining and Metallurgy, London, pp. 91–101.

Boler, FM & Swanson, PL 1993, 'Modelling of a destress blast and subsequent seismicity and stress changes', *Proceedings of the 3rd International Conference on Rockbursts and Seismicity in Mines*, in RP Young (ed.), A.A. Balkema, Rotterdam, pp. 35–40.

Borg, T 1988, *Ortdrivning med avlastningssprängning; Bergmekanisk uppföljning på 815 m nivån i Malmberget* (Local driving with relief blasting; Rock mechanical follow-up at the 815 m level in Malmberget), report BeFo 331:1/88, SveDeFo 1989:1.

Corp, EL 1980, 'Rock mechanics research in the Coeur d'Alene mining district', in O Stephansson and MJ Jones (eds), *Proceedings of the Conference on Application of Rock Mechanics to Cut-and-Fill Mining*, University of Luleå, Luleå, pp. 271–297.

Cullen, M 1988, *Studies of destress blasting at Campbell Red Lake Mine*, MSc thesis, McGill University, Montréal.

Fairhurst, C 2017, 'Some challenges of deep mining', *Engineering,* vol. 3, pp. 527–537, https://doi.org/10.1016/J.ENG.2017.04.017.

Grodner, M 1999, 'Fracturing around a preconditioned deep level gold mine stope', *Geotechnical and Geological Engineering*, vol. 17, pp. 291–304, https://doi.org/10.1023/A:1008977609619

Hanson, D, Quesnel, W & Hong, R 1987, *De-stressing a Rockburst-prone Crown Pillar – Macassa Mine*, CANMET, Mining Research Laboratories, Report MRL 87-82 (TR), Elliot Lake.

Hashemi, AS & Katsabanis, P 2021, 'Tunnel face preconditioning using destress blasting in deep underground excavations', *Tunnelling and Underground Space Technology*, vol. 117, pp. 104–126, https://doi.org/10.1016/j.tust.2021.104126

Hedley, DGF 1992, *Rockburst Handbook for Ontario Hardrock Mines*, CANMET Special Report SP92-1E, Energy, Mines and Resources, Canada Center for Mineral and Energy Technology, Toronto.

Hedley, DGF & Udd, JE 1989, 'The Canada-Ontario-industry rockburst project', *Pure and Applied Geophysics*, vol. 129, pp. 661–672, http://dx.doi.org/10.1007/BF00874531

Hoek ,E & Brown, ET 1997, 'Practical estimates of rock mass strength', *International Journal of Rock Mechanics and Mining Sciences and Geomechanics Abstracts*, vol. 34, no. 8, pp. 1165-–1186.

Hoek, E & Diederichs, MS 2006, 'Empirical estimation of rock mass modulus'*, International Journal of Rock Mechanics and Mining Sciences*, vol. 43, no. 2, pp. 203–215.

Hoek, E, Carranza-Torres, CT & Corkum, B 2002, 'Hoek-Brown failure criterion-2002 edition', *Rock Mechanics: Proceedings of the Fifth Symposium on Rock Mechanics*, University of Toronto Press, Toronto. pp. 267–273.

Itasca Consulting Group, Inc. 2019, *FLAC3D – Fast Lagrangian Analysis of Continua in Three Dimensions*, version 7, computer software.

James, JV 1998 *Geotechnical Influences Upon the Design and Operation of a Deep Level Wide Orebody Gold Mine*, PhD thesis, University of Wales, College of Cardiff.

Jessu, KV, Spearing, AS & Sharifzadeh, M 2018, 'A parametric study of blast damage on hard rock pillar strength', *Energies* vol. 11, no. 7, pp. 1900–1917, https://doi.org/10.3390/en11071901

Karwoski, WJ, McLaughin, WC, Blake, W 1979, *Rock Preconditioning to Prevent Rockbursts: Report on a Field Demonstration*, *Report of Investigations 8381*, Department of the Interior, Bureau of Mines, Washington, DC.

Kang, H, Lv, H, Gao, F, Meng ,X, Feng, Y 2018 'Understanding mechanisms of de-stressing mining-induced stresses using hydraulic fracturing', *International Journal of Coal Geology,* vol. 196, pp. 19–28, https://doi.org/10.1016/j.coal.2018.06.023

Konicek, P & Waclawik, P 2018 'Stress changes and seismicity monitoring of hard coal longwall mining in high rockburst risk areas', *Tunnelling and Undergr Space Technology*, vol. 81, pp. 237-251, https://doi.org/10.1016/j.tust.2018.07.019

Konicek P, Ptáček J, Staš L, Kukutsch R, Waclawik, P & Mazaira, A 2014, 'Impact of destress blasting on stress field development ahead of a hardcoal longwall face', in R Alejano, Á Perucho, C Olalla, R Jiménez (eds.) *Rock Engineering and Rock Mechanics: Structures in and on Rock Masses - Proceedings of EUROCK 2014, ISRM European Regional Symposium*, CRC Press, Boca Raton, pp. 585–590.

Konicek, P, Schreiber, J & Nazarova, L 2019, 'Volumetric changes in the focal areas of seismic events corresponding to destress blasting', *International Journal of Mining Science and Technology*, vol. 29, pp. 541–547, https://doi.org/10.1016/j.ijmst.2019.06.004

Krauland, N & Söder, PE 1988, *Bergstabilisering Genom Avlastningssprängning – Erfarenheter Från Bolidens Gruvor* (Rock Stabilisation by De-Stress Blasting – Experiences From Boliden Mines), paper presented at Rock Mechanics Meeting, Stockholm, pp. 137–160.

Makuch A, Neumann, M, Hedley, DGF & Blake, W 1987, *Destress Blasting at Campbell Red Lake Mine*, Report SP 87–88E, CANMET, Elliot Lake Laboratory.

Malan, DF & Spottiswoode, SM 1997, Time-dependent fracture zone behavior and seismicity surrounding deep level stopping operations, in SJ Gibowicz and S Lasocki (eds), *Rockbursts and Seismicity in Mines 97: Proceedings of the 4th International Symposium*, AA Balkema, Rotterdam, pp 173–177.

McMahon, T 1988, *Rock Burst Research and the Coeur d'Alene District*, US Bureau of Mines Information, Circular 9186, Washington, DC.

Mikula, PA & Lee, MF 2002, 'Forecasting and controlling pillar instability at Mt Charlotte Mine', *Proceedings of the 1st International Seminar on Deep and High Stress Mining*, Australian Centre for Geomechanics, Perth.

Mikula , PA, Lee, MF & Guilfoyle, K 1995, 'Preconditioning a large pillar at Mt Charlotte Mine', *Underground Operators Conference*, pp. 265–272.

Mikula, PA, Sharrock, G, Lee, MF & Kinnersly, E 2005, 'Seismicity management using tight slot blasting for stress control at Mt Charlotte Mine', in Y Potvin & M Hudyma (eds), *RaSiM6: Proceedings of the Sixth International Symposium on Rockburst and Seismicity in Mines Proceedings*, Australian Centre for Geomechanics, Perth, pp. 401–408, https://doi.org/10.36487/ACG_repo/574_41

Mitri, HS 2000, *Practitioner's Guide to Destress Blasting in Hard Rock Mines*, technical report, McGill University, Montréal.

Mitri, HS, Scoble, MJ & McNamara, K 1988, Numerical studies of de-stressing mine pillars in highly stressed rock, *Proceedings of the 41st Canadian Geotechnical Conference*, Canadian Geotechnical Society, pp. 50–56.

Mitri, H, Tang, B, Marwan , J, Comeau, W 2000, 'Tunnel face de-stressing in burst-prone rock', *Canadian Tunnelling Journal*, pp. 131–142.

Momoh, OA, Mitri, HS, Rizkalla, MK 1996, 'Numerical modelling of destress blasting', in M Aubertin, F Hassani, HS Mitri (eds) *Proceedings of 2nd North American Rock Mechanics Symposium: NARMS '96*, A.A. Balkema, Rotterdam.

Russo, A & Hormazabal, E 2019, 'Correlations between various rock mass classification systems, including Laubscher (MRMR), Bieniawski (RMR), Barton (Q) and Hoek and Marinos (GSI) Systems', *Geotechnical Engineering in the XXI Century: Lessons Learned and Future Challenges*, IOS Press, London, pp 2806–2815.

Saharan, MR 2004, *Dynamic Modelling of Rock Fracturing by Destress Blasting*, PhD thesis, McGill University, Montréal.

Saiang, D & Nordlund, E 2005, *De-stressing and Preconditioning of Rock*, Gallivare Hard Rock Research, Gallivare, https://urn.kb.se/resolve?urn=urn:nbn:se:ltu:diva-22200

Scoble, MJ, Cullen, M & Makuch, A 1987, 'Experimental studies of factors relating to destress blasting', in IW Farmer, JJ Daemen, CS, Desai, CE Glass & SP Neuman (eds), *Rock Mechanics: Proceedings of the 28th US Symposium*, A.A Balkema, Rotterdam, pp. 901–908.

Sellers, EJ 2011, 'Controlled blasting for enhanced safety in the underground environment', *Journal of the Southern African Institute of Mining and Metallurgy,* vol. 111, no. 1, pp. 11–17.

Sengani, F & Amponsah-Dacosta, F 2018, 'The application of the face-perpendicular preconditioning technique for de-stressing seismically active geological structures', *Mining Technology*, vol. 127, no. 4, pp. 241–255. https://doi.org/10.1080/25726668.2018.1497871

Sengani, F & Zvarivadza, T 2018, 'The implementation of de-stress gold mining technique along complex geological structures and heavily fractured ground conditions', in V Litvinenko (ed.), *Geomechanics and Geodynamics of Rock Masses: Proceedings of the 2018 European Rock Mechanics Symposium*, CRC Press, Boca Raton.

Sengani, F, Zvarivadza, T & Adoko, AC 2019, 'Comparison of two adopted face perpendicular preconditioning techniques', *Mining Technology*, vol. 128, no. 1, pp. 21–38, https://doi.org/10.1080/25726668.2018.1517204.

Shnorhokian, S & Ahmed ,S 2024, 'Mechanisms and measurements of de-stressing in underground mines: a state-of-the-art review', *Mining, Metallurgy & Exploration*, in press.

Swedberg, E, Boeg-Jensen, P, Andersson, U & Rutanen, H 2018, *Results Summary of Phase 1 Hydraulic Fracturing Trial in the Kiirunavaara Mine*, LKAB investigation.

Tang, BY 2000, *Rockburst Control Using Destress Blasting*, PhD thesis, McGill University, Montreal.

Tang, B & Mitri, HS 2001, 'Numerical modelling of rock preconditioning by destress blasting', *Proceedings of the Institution of Civil Engineers - Ground Improvement*, vol. 5, no. 2, pp. 57-67.

Toper, AZ, Grodner, M & Lightfoot, N 1997, 'Preconditioning: a rockburst control technique', in SJ Gibowicz & S Lasocki (eds), *4th International Symposium on Rockbursts and Seismicity in Mines*, CRC Press, pp. 267–272.

Toper, AZ, Stewart, RD, Kullmann, DH, Grodner, M, Lightfoot, N, Janse van Rensburg, AL & Longmore, PJ 1998 *Develop and Implement Preconditioning Techniques to Control Face Ejection Rockbursts for Safer Mining in Seismically Hazardous Areas*, Safety in Mines Research Advisory Committee, GAP 336.

Torbica, S & Lapčević, V 2015, 'Estimating extent and properties of blast-damaged zone around underground excavations', *REM: Revista Escola de Minas,* vol. 68, no. 4, pp. 441–453, https://doi.org/10.1590/0370-44672015680062

Vennes, I & Mitri, HS 2017, 'Geomechanical effects of stress shadow created by large-scale destress blasting', *Journal of Rock Mechanics and Geotechnical Engineering*, vol. 9, no. 6, pp. 1085–1093, https://doi.org/10.1016/j.jrmge.2017.09.004

Vennes, I, Mitri, HS, Chinnasane, D & Yao M 2020, 'Large-scale destress blasting for seismicity control in hard rock mines: a case study', *International Journal of Mining Science and Technology* vol. 30, no. 2, pp. 141–149.

Vlachopoulos, N & Diederichs, MS 2014, 'Appropriate uses and practical limitations of 2D numerical analysis of tunnels and tunnel support response', *Geotechnical and Geological Engineering*, vol. 32, no. 2, pp. 469–488.

Wagner, H 2019, 'Deep mining: a rock engineering challenge', *Rock Mechanics and Rock Engineering*, vol. 52, pp. 1417–1446, https://doi.org/10.1007/s00603-019-01799-4

Wiles, TD & MacDonald, P 1988, 'Correlation of stress analysis results with visual and microseismic monitoring at Creighton mine', *Computers and Geotechics*, vol. 5, no. 2, pp. 105–121.

Whittaker, BN & Reddish, DJ 1990, 'Mine opening stability aspects in relation to deep-level mining', in DAI Ross-Watt & PDK Robinson (eds), *International Deep Mining Conference: Volume 2 Technical Challenges in Deep Level Mining*, The South African Institute of Mining and Metallurgy, Johannesburg, pp. 1119–1122.

Willan, J, Scoble, M & Pakalnis, V 1985, 'De-stressing practice in rockburst-prone ground', in SS, Peng & JH, Kelley (eds), *Proceedings of the Fourth Conference on Ground Control in Mining (ICGCM),* Department of Mining Engineering, West Virginia University, Morgantown, pp. 135–147.

Yu, S, Yang, X, Zhu, C, Yuan, Y & Wang, Z 2021, 'De-stressing mechanics effect of surrounding rock induced by blasting precondition at deep drift development', *Geotechnical and Geological Engineering*, vol. 39, pp. 4113–4125, https://doi.org/10.1007/s10706-021-01687-1

Zhu, WC, Wei, CH, Li, S, Wei, J & Zhang, MS 2013, 'Numerical modeling on destress blasting in coal seam for enhancing gas drainage', *International Journal of Rock Mechanics and Mining Sciences*, vol. 59, pp. 179–190, https://doi.org/10.1016/j.ijrmms.2012.11.004